RAPID COMMUNICATIONS

PHYSICAL REVIEW B VOLUME 47, NUMBER 11 15 MARCH 1993-I

Raman scattering and collective excitations in doped tunneling semiconductor superlattices

Xiaoju Wu and Sergio E. Ulloa

Department of Physics and Astronomy and Condensed Matter and Surface Sciences Program, Ohio University, Athens, Ohio 45701-2979

(Received 21 September 1992)

We present a theoretical study of the electronic excitations in doped *tunneling* semiconductor superlattices of finite size. Raman scattering yields are obtained from the density-density response function, providing mode dispersion relations *and* relative intensities. We find that as the intraminiband and interminiband plasma modes carry most of the oscillator strength, other single-particle-like excitations have nonvanishing intensities as well. Strong surface-related modes, associated with charge depletion near the surface layers, are shown for finite wavelengths. The intraminiband plasma mode exhibits a two-dimensional-like behavior for long wavelengths, and carries most of the oscillator strength for short ones, while one of the surface modes shows a nearly linear dispersion relation. A novel tunneling mode has nonzero frequency and strength as the wave vector approaches zero.

Advances in materials growth, such as molecular-beam epitaxy, have made possible the growth of semiconductor superlattices consisting of an alternating sequence of thin layers, such as in the $GaAs/Al_xGa_{1-x}As$ system. These structures have attracted much attention in recent years due to their tunable electronic properties and potential applications on new electronic devices.[1] The electronic properties of these superlattices have been investigated extensively by experimental techniques such as interband optical absorption, infrared scattering, electron tunneling, and magnetotransport.[1] Inelastic light (Raman) scattering has been particularly useful in the study of single-particle and collective excitations, as it has provided a great deal of information on the rich structures of these semiconductor systems.[2] More recently, this technique has also been used in the investigation of electronic excitations in systems of highly reduced dimensionality.[3]

Most theoretical studies on superlattice systems have adopted a so-called flat miniband model, in which the charge carriers are assumed to be completely confined into separate quantum wells. Inelastic light scattering intensities from a semi-infinite array of such two-dimensional electron-gas layers were calculated in the pioneering work of Jain and Allen,[4] although in the diagonal approximation, where intersubband transitions are neglected for simplicity. Hawrylak and co-workers[5] have calculated the Raman yields for semi-infinite and finite quantum-well arrays, including intersubband effects, although still in the flat miniband (no-tunneling) configuration. On the other hand, Katayama and Ando[6] have also presented self-consistent calculations for the ground state and excitations of an infinite multiple-quantum-well system, so that surface modes were not included, and dispersion relations were not presented. Using d-parameter theory, Zhang, Ulloa, and Schaich[7] have investigated the collective modes of a *tunneling* superlattice of finite size in the long-wavelength limit, showing the appearance of tunneling and surface modes. As the wave vector increases, the frequency of the different modes is expected to change since the electron layers in the finite superlattice cease to respond in phase, affecting the depolarization fields induced in this interacting system. One would expect strong mode dispersion, and even the possible appearance of new modes in the system, for nonzero wave numbers. The behavior of collective modes in this system in the finite wavelength regime is presented in this Rapid Communication. We present results for Raman scattering intensities for varying momentum transfer, providing a systematic description of the dispersion relations and relative oscillator strengths of the different modes in the system.

Our calculations include *tunneling*, *intersubband coupling*, and the effects of finite superlattice length, which also include the effects of the strong *charge depletion* in real structures due to Fermi-level pinning to mid-band-gap levels.[8] We find that, in addition to the expected series of intraminiband and interminiband plasma modes in the infinite ("bulk") system there also exist several surface-related modes. All the modes are strongly dispersed as the momentum transfer parallel to the superlattice surface $q_{\|}$ changes. The intraminiband bulk plasma mode exhibits a two-dimensional (2D) -like behavior in the long wavelength regime ($\omega \propto \sqrt{q_{\|}}$), while a *surface plasma mode* has a nearly linear dispersion relation due to the drastic change of carrier density in the surface layers of the superlattice. This surface mode disappears in the infinite wavelength limit.[7] Furthermore, our calculations show a *tunneling mode*, associated with the carrier motion along the superlattice growth direction, with a finite excitation energy and progressively stronger as $q_{\|}$ approaches zero. We also find that the bulk interminiband mode has a dispersion relation with negative slope in the small-wave-vector region, in agreement with previous calculations,[9] and that its oscillator strength decreases rapidly for larger $q_{\|}$, a somewhat unexpected result.

We consider a doped semiconductor superlattice as N quantum wells of width a separated by a series of finite potential barriers of thickness b, which allow carrier tunneling from well to well, and are deposited on a semi-infinite uniform medium with a dielectric constant ϵ. The electronic motion parallel to the surface is assumed free-like, with an overall density profile in the perpendicular direction, calculated self-consistently, to account for the surface depletion appearing due to Fermi-level pinning.[8] The resulting level structure consists of a series of closely spaced levels, reminiscent of the minibands in the infinite system, together with surface *Tamm-like* states lying in the miniband gaps and with localized wave functions.[8]

The differential cross section due to charge-density excitations is proportional to the loss function $P(\omega, \mathbf{Q})$ for a fixed polarization.[4–6] If the incoming and scattered light have frequencies and wave vectors $(\omega_i, \mathbf{q}_i, k_z^i)$ and $(\omega_s, \mathbf{q}_s, -k_z^s)$, respectively, the loss function is related to the density-density correlation function $\chi(q_\parallel, \omega, z, z')$ by[4–6] $P(\omega, \mathbf{Q}) = \int P(\omega, \mathbf{Q}, z)\, dz$, where

$$P(\omega, \mathbf{Q}, z) = e^{-ik_z^* z} \int dz'\, e^{ik_z z'}\, [-\mathrm{Im}\chi(q_\parallel, \omega, z, z')], \tag{1}$$

$\omega = \omega_i - \omega_s$, and $\mathbf{Q} = (\mathbf{q}_\parallel, k_z) \equiv (\mathbf{q}_i - \mathbf{q}_s, k_z^i + k_z^s)$. $P(\omega, \mathbf{Q}, z)$ is the contribution to the total Raman scattering intensity from the electron "layer" at position z and for given $(\omega, \mathbf{Q})$. The commonly used substitution,[4–6] $k_z^i = k_z^s = k + i/2\lambda$, where $kc = \omega_i \mathrm{Re}\sqrt{\epsilon}$, and $c/\lambda = 2\omega_i \mathrm{Im}\sqrt{\epsilon}$, reflects the near specular geometry used in typical experiments. The density-density correlation function is obtained from a fully nonlocal microscopic response theory within the random-phase approximation.[10] This calculation is performed using a basis set of localized Wannier functions for different minibands.[8] The wave function for the nth eigenstate for motion along the superlattice growth (z) direction is written as $\Phi_n(z) = \sum_{j,\alpha} b_{j\alpha}^n \phi_j^\alpha(z)$, where $\phi_j^\alpha(z)$ is the Wannier function for the αth miniband centered at the jth quantum well. The self-consistent linear response formalism leads to[7] $\chi(q_\parallel, \omega, z, z') = \hat{\mathbf{A}}^t(z) \cdot [\hat{\mathbf{B}}(\mathbf{1} - \hat{\mathbf{V}}\hat{\mathbf{B}})^{-1}] \cdot \hat{\mathbf{A}}(z')$, where the $\hat{\mathbf{A}}$ vector and various matrix elements are given by $\hat{\mathbf{A}}_s(z) = \phi_i^\alpha(z)\, \phi_j^\beta(z)$, $\hat{\mathbf{B}}_{ss'}(\mathbf{q}_\parallel, \omega) = \sum_{nn'} b_{i\alpha}^n b_{j\beta}^{n'} \Pi_{nn'} b_{j'\alpha'}^n b_{j'\beta'}^{n'}$, and

$$\hat{\mathbf{V}}_{s,s'}(q_\parallel) = \int\int dz\, dz'\, \hat{\mathbf{A}}_s(z) V(q_\parallel, z, z') \hat{\mathbf{A}}_{s'}(z'). \tag{2}$$

Here, $s = (\alpha, i, \beta, j)$ is a compound index,

$$V(q_\parallel, z, z') = \frac{2\pi e^2}{\epsilon q_\parallel} e^{-q_\parallel |z - z'|} + \frac{2\pi e^2}{\epsilon q_\parallel} \frac{\epsilon - 1}{\epsilon + 1} e^{-q_\parallel (z + z')} \tag{3}$$

is the 2D Fourier component of the Coulomb interaction (including image charge effects in the second term), and $\Pi_{nn'}$ is the well-known 2D Lindhard polarization, generalized to include interlevel transitions between states n and n'. $\Pi_{nn'}$ is evaluated in a closed form using contour integration,[11] completing the set of equations for the calculation of χ and P in Eq. (1).

Here, we present results for a ten-period $GaAs/Al_xGa_{1-x}As$ superlattice deposited on a semi-infinite substrate with the same dielectric constant as the superlattice layers, $\epsilon = 12.5$.[8,12] The period of the superlattice and doping density are taken to be $d = a + b = 226$ Å and $\rho = 1.9 \times 10^{17}$ cm^{-3}, respectively. The phenomenological level broadening parameter η is taken as $\eta \approx 0.5$ meV, and $kd = 0.2$. Energy levels and corresponding wave functions are calculated using a tight-binding envelope-function approximation, and the potential associated with the carrier-depletion profiles is calculated self-consistently in a two-miniband model.[8] The resulting levels are clustered into two groups of four and five states, respectively, with wave functions extended throughout the ten-layer structure, and forming incipient minibands in this finite-size system. Moreover, there are also a series of surface-localized states detached from the miniband groups, and lying in the miniband gaps. Only one of these surface states is partially populated at this doping level and gives rise to a series of interesting surface-localized excitations, as we discuss below.[7,8]

Figure 1 shows the loss function versus frequency for several typical wave vectors. In the wave vector regime $q_\parallel \geq 0.2$ (wave vectors are given in multiples of $q_0 = 2\pi \times 10^{-3}$ Å^{-1}), three prominent intraminiband plasma modes are seen with energy below 20 meV, as well as two interminiband modes at $\omega \approx 40$ meV. As the wave vector decreases from $q_\parallel = 0.2$, one more intraminiband mode appears at $\omega \approx 9$ meV, as the increasing weight of vertical transitions make this surface-to-bulk excitation more evident (see below).

To identify the nature of the different modes in the system, the z-dependent intensity function $P(\omega, q_\parallel, z)$ is calculated. In Fig. 2 we show results for $q_\parallel = 0.25$, where each curve corresponds to a different frequency mode as indicated. Since $P(\omega, q_\parallel, z)$ is the contribution to the total intensity $P(\omega, q_\parallel)$, Fig. 2 describes the amplitude of the given mode along the z direction, while propagating along the superlattice planes with $(\omega, q_\parallel)$. Moreover, one

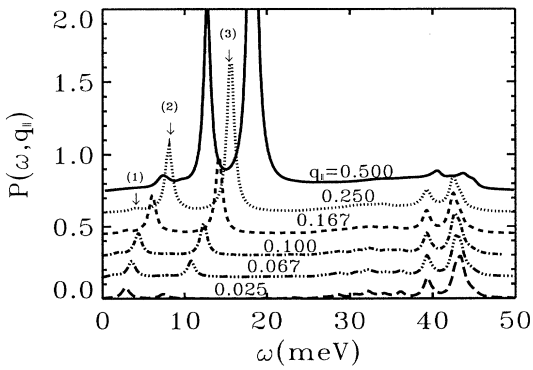

FIG. 1. Raman-scattering intensities for various parallel momentum transfer values (in units of $q_0 = 2\pi \times 10^{-3}$ Å^{-1}). Each curve is displaced vertically for clarity. Intensity is plotted in arbitrary units. Peaks below (above) 25 meV are intraminiband (interminiband) modes.

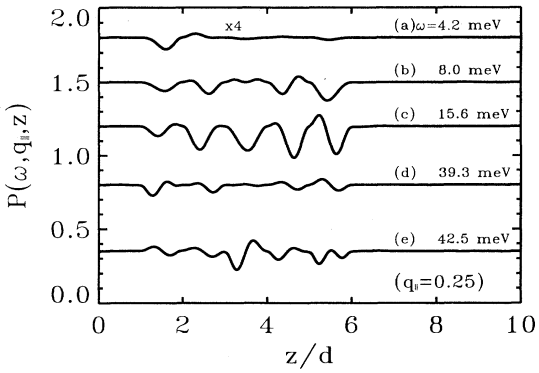

FIG. 2. Raman-scattering amplitudes from different electron "z layers" along superlattice growth direction for $q_{\|} = 0.25q_0$. Each curve corresponds to different frequency mode as indicated. Intensity shown in arbitrary units.

can also trace the peak positions in Fig. 1 as function of the parallel momentum transfer, obtaining the dispersion relation for each mode. This completes the physical description of the modes in the structure.

Curve (a) in Fig. 2 indicates that the first mode in the Raman scattering intensity curves [peak (1) in Fig. 1] is strongly localized in the surface layers. This mode is then associated with the motion of the electrons on the surface along the layer planes, while the interior "bulk" layers remain nearly immobile. This surface in-plane motion mode exhibits a nearly linear dispersion relation (× in Fig. 3). A similar "acoustic" mode has been found theoretically [via calculations of the inelastic electron-scattering (IES) yield[13]] in systems such as ZnO, and InAs(110),[14] and observed experimentally in quantum-well systems.[2] As $q_{\|}$ decreases, the excitation energy of the surface mode approaches zero, indicating a weaker interaction between the electrons in the 2D-like surface layer moving independently of the bulk. Notice that the intensity of this mode also vanishes as the wave vector

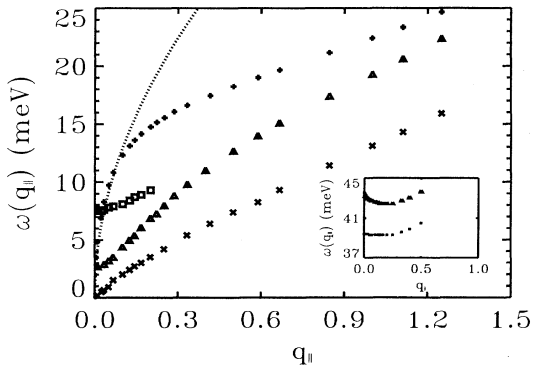

FIG. 3. Dispersion relations for different modes in Fig. 1. *Intraminiband* plasma modes: surface [×, peak (1) in Fig. 1], tunneling [△, peak (2)], and bulk [+, peak (3)] modes. □ is surface-to-miniband transition. *Interminiband* modes shown in inset. Low (high) -energy curve is surface-related (bulk) mode.

approaches zero. This general behavior agrees with IES yield calculation results for this system.[15]

Mode (b) in Fig. 2 [peak (2) in Fig. 1] carries a large portion of the total oscillation strength in the intensity curve, and is called a *tunneling mode*. This is associated with the tunneling motion of the electrons along the superlattice growth direction.[7,16] In terms of energy levels, this mode corresponds to transitions among the bulk-related subbands which form the lowest miniband. This mode reaches a *finite* value of 2.8 meV as $q_{\|}$ goes to zero, a value proportional to the bandwidth and other structural parameters.[7,16] The d-parameter theory[7] and IES calculations[15] give similar results. As $q_{\|}$ increases to about 1.3, this mode enters the Landau damping regime, it exchanges energy with the single-particle excitations, and becomes broad and not well defined. The dispersion relation for this mode is also shown in Fig. 3 (△ curve).

The third mode [peak (3) in Fig. 1] extends throughout the superlattice, as seen in curve (c) in Fig. 2, and carries most of the intensity at large wave vectors.

Classically, this intraminiband bulk plasma mode can be viewed as the in-phase motion of *all* the electrons in the system moving parallel to the surface. Its dispersion relation is shown by the + curve in Fig. 3. For comparison, the dispersion relation for an ideal 2D electron gas[1] (2DEG) is also plotted in Fig. 3 (dotted curve), $\omega(q_{\|}) = [4\pi ne^2 q_{\|}/(\epsilon+1)m]^{1/2}$, where n is the 2D electron number density. For wave vectors smaller than 0.1, equivalent to a wavelength of five times the total superlattice length, the dispersion of this "bulk" mode follows closely the ideal 2DEG mode. However, as $q_{\|}$ increases, the "internal structure" of the superlattice makes this mode depart from a 2D-like behavior, as one would anticipate.

Our calculations also show a distinct mode weakly appearing as the wave vector decreases below 0.2 (□ in Fig. 3). This mode corresponds to the transition from the highest occupied bulk subband state to the partially occupied surface state. The function $P(\omega, q_{\|}, z)$ for this mode shows it is basically localized in the surface layers (not shown in Fig. 2). Moreover, as $q_{\|}$ decreases the oscillator strength of this mode is increasingly stronger and the energy approaches 7.8 meV for $q_{\|} \to 0$, which can be identified as the single-particle transition energy of 7.2 meV shifted by Coulomb depolarization effects.[5–7] The $q_{\|} = 0$ limit of this mode is also found by Zhang, Ulloa, and Schaich in their d-parameter calculations.[7]

The two interminiband plasma modes in Fig. 1 lie above the anticipated interminiband single-particle transition range (between 20 and 38 meV), due to depolarization shifts.[5–7] (Notice in Fig. 1 that single-particle features in this window have nonzero strength only for small $q_{\|}$ and become rather broad at large $q_{\|}$.) The two interminiband modes dominate the spectrum for small wave vectors ($q_{\|} \leq 0.025$). However, the decreasing importance of vertical transitions for larger $q_{\|}$ lead to the weakening of these two modes, relative to the intraminiband features. This interesting shift in the oscillator strengths is quite unexpected, and should be easily discernible in experiments. Curves (d) and (e) in Fig. 2 indicate that

the lower (or higher) interminiband mode is associated with the collective transitions from the occupied surface (or bulk) subband to the empty subbands. Their dispersion relations are given in the inset of Fig. 3. In the region $q_{\|} \leq 0.25$, the energy of the surface-related mode remains nearly constant, while the bulk-associated mode exhibits a strong dispersion relation with negative slope, as obtained in other calculations for a 2D electron gas,[11] and a superlattice system.[9,15] As $q_{\|} \rightarrow 0$, these modes approach 39.4 and 43 meV, respectively, which agrees with our IES results (39.4 and 42.4 meV),[15] and with infrared absorption results (39.8 and 42.5 meV).[7]

In summary, we have investigated Raman-active excitations in doped tunneling semiconductor superlattices with depletion layers. Our calculation is based on a fully nonlocal microscopic linear response theory. Surface and tunneling modes are shown to exist for different wave vectors. Even though plasma modes carry most of the oscillator strength, the single-particle-like excitations have also appreciable weight, especially at low wave numbers. We hope the results presented in this paper would stimulate further interest in these systems.

We thank Professor W. L. Schaich for his encouragement and extensive discussions. Calculations were performed on the Cray Y/MP at the Ohio Supercomputer Center. This project was supported by the U.S. Department of Energy, Grant No. DE-FG02-91ER45334.

[1] T. Ando, A. B. Fowler, and F. Stern, Rev. Mod. Phys. **54**, 437 (1982); P. J. Stiles, in *Interfaces, Quantum Wells and Superlattices*, Vol. 179 of *NATO Advanced Study Institute, Series B: Physics*, edited by C. R. Leavens and R. Taylor (Plenum, New York, 1988).

[2] R. Sooryakumar, A. Pinczuk, A. Gossard, and W. Wiegmann, Phys. Rev. B **31**, 2578 (1985); A. Pinczuk, M. G. Lamont, and A. C. Gossard, Phys. Rev. Lett. **56**, 2092 (1986); J. Menendez, A. Pinczuk, J. P. Valladares, L. N. Pfeiffer, K. W. West, A. C. Gossard, and J. H. English, Surf. Sci. **228**, 65 (1990); M. Dutta, D. D. Smith, P. G. Newman, X. C. Liu, and A. Petrou, Phys. Rev. B **42**, 1474 (1990); B. Jusserand, D. Richards, B. Etienne, H. Peric, and G. Fasol, Surf. Sci. **263**, 527 (1992).

[3] A. Pinczuk, S. Schmitt-Rink, G. Danan, J. P. Valladares, L. N. Pfeiffer, and K. W. West, Phys. Rev. Lett. **63**, 1633 (1989); J. S. Weiner, D. Danan, A. Pinczuk, J. Valladares, L. N. Pfeiffer, and K. West, *ibid.* **63**, 1641 (1989); A. R. Goñi, A. Pinczuk, J. S. Weiner, J. M. Calleja, B. S. Dennis, L. N. Pfeiffer, and K. W. West, *ibid.* **67**, 3298 (1991).

[4] J. K. Jain and P. B. Allen, Phys. Rev. Lett. **54**, 947 (1984); Phys. Rev. B **32**, 997 (1985).

[5] P. Hawrylak, J. W. Wu, and J. J. Quinn, Phys. Rev. B **32**, 5169 (1985); G. Eliasson, P. Hawrylak, and J. J. Quinn, *ibid.* **35**, 5569 (1987).

[6] S. Katayama and T. Ando, J. Phys. Soc. Jpn. **54**, 1615 (1985).

[7] J. Zhang, S. E. Ulloa, and W. L. Schaich Phys. Rev. B **41**, 5467 (1990); **43**, 9864 (1991).

[8] J. Zhang and S. E. Ulloa, Phys. Rev. B **38**, 2063 (1988); Solid State Commun. **71**, 643 (1989); Y. S. Joe and S. E. Ulloa, J. Phys. Condens. Matter **2**, 7137 (1990).

[9] A. C. Tselis and J. J. Quinn, Phys. Rev. B **29**, 3318 (1984).

[10] Exchange effects ignored by the random-phase approximation have been shown to yield only a small shift of the electronic features in these systems (Refs. 5–7). The larger effects of exchange and correlation in highly confined nearly-two-dimensional systems [see Gammon *et al.*, Phys. Rev. Lett. **68**, 1884 (1992)] are nearly suppressed in the type of thin barrier system considered here, since carriers are much less confined. Phonon effects have also been neglected, as the main optical frequency does not overlap strongly with the electronic transitions, for the parameters used here. Inclusion of these effects is straightforward and anticipated to produce small mode shifts and/or mixing (see Ref. 7).

[11] F. Stern, Phys. Rev. Lett. **18**, 546 (1967); L. Wendler and R. Pechstedt, Phys. Status Solidi B **138**, 197 (1986).

[12] H. L. Störmer, J. P. Eisenstein, A. C. Gossard, W. Wiegmann, and K. Baldwin, Phys. Rev. Lett. **56**, 85 (1986).

[13] D. H. Ehlers and D. L. Mills, Phys. Rev. B **36**, 1051 (1987).

[14] H. Yu and J. C. Hermanson, Phys. Rev. B **41**, 5991 (1990); **40**, 11 851 (1989).

[15] Xiaoju Wu and S. E. Ulloa (unpublished).

[16] X. Zhu, X. Xia, J. J. Quinn, and P. Hawrylak, Phys. Rev. B **38**, 5617 (1988).